

SCIENTIFIC REPORTS



OPEN

Layered polymeric nitrogen in RbN_3 at high pressures

Xiaoli Wang^{1,2}, Jianfu Li³, Ning Xu⁴, Hongyang Zhu⁵, Ziyu Hu² & Li Chen¹

Received: 05 August 2015

Accepted: 14 October 2015

Published: 13 November 2015

The structural evolutionary behaviors of nitrogen in RbN_3 have been studied up to 300 GPa using a particle swarm optimization structure searching method combined with density functional calculations. Three stable new phases with *P*-1, *P6/mmm* and *C2/m* structure at pressure of 30, 50 and 200 GPa are identified for the first time. The analysis of the crystal structures of three new predicted phases reveals that the transition of N_3^- ions goes from linear molecules to polymeric chains, benzene-like rings and then to polymeric layers induced by pressure. The electronic structures of three predicted phases reveal that the structural changes are accompanied and driven by the change of orbital hybridization of N atoms from *sp* to *sp*² and finally to partial *sp*³. Most interestingly, the Rb atoms show obvious transition metal-like properties through the occupation of 4*d* orbitals in high-pressure phases. Moreover, the Rb atoms are characterized by strong hybridization between 4*d* orbitals of Rb and 2*p* orbitals of N in *C2/m* structure. Our studies complete the structural evolution of RbN_3 under pressure and reveal for the first time that the Rb atoms in rubidium nitride possess transition element-like properties under pressure.

Metal azides have been the subjects of many studies including their structural stability, lattice dynamics, electronic structure, and many other physical properties because of their linear azide anion¹, as well as their significant industrial importance as gas generators and explosives². Recently, taking metal azides as starting materials to synthesis polymeric nitrogen, a potential high-energy-density-material, has become a new topic due to the potential lower synthesis pressure compared with pure nitrogen gas. In nitrogen gas, nitrogen exists in N_2 molecules and the connection between nitrogen atoms is triple bonds $\text{N}\equiv\text{N}$. In metal azides, nitrogen exists in N_3^- anions and the nitrogen atoms are connected through double bonds $\text{N}=\text{N}$. It is expected that the N_3^- anions in metal azides may form a polymeric nitrogen network more readily than N_2 molecules, since the $\text{N}=\text{N}$ have a much lower bonding energy (418 KJ/mol) than the $\text{N}\equiv\text{N}$ (954 KJ/mol). Under pressure, N_3^- anion will undergo a series of structural transitions accompanied by the change of hybridization type of nitrogen atoms, as shown in Fig. 1. Under low pressure, usually fewer than 30 GPa, N_3^- anions maintains their linear structures with *sp* hybridization, in which the crystal maybe undergo orientational phase transition of N_3^- anions induced by pressure^{3–7}. As pressure increase, N_3^- anions translates to a so called pseudo-benzene N_6 ring with *sp*² hybridization^{4,5,8,9}. Continuing to increase pressure, nitrogen will form polymeric structure with partial *sp*³ hybridization. For CsN_3 , our previous work indicates that N_3^- anions will translate to a chain like structure at 51 GPa instead of N_6 ring¹⁰. In the process of nitrogen structural transition, alkali metal atoms in azides act as electronic donors to change the connection between nitrogen atoms and electronic properties of compounds. A lot of experimental and theoretical work has been done to study the high-pressure behaviors of nitrogen in LiN_3 ^{4,8,11–15}, NaN_3 ^{3,5,16}, KN_3 ^{7,9,14,17–21}, and CsN_3 ^{10,22}. Therefore, a study of the high-pressure behavior of RbN_3 would provide more insights into the mechanism of pressure-induced structural

¹Institute of Condensed Matter Physics, Linyi University, Linyi 276005, P. R. China. ²Beijing Computational Science Research Center, Beijing, 100084, P. R. China. ³School of science, Linyi University, Linyi 276005, P. R. China. ⁴Department of Physics, Yancheng Institute of Technology, Yancheng 224051, China. ⁵State Key Laboratory of Superhard Materials, College of Physics, Jilin University, Changchun 130012, P. R. China. Correspondence and requests for materials should be addressed to J.L. (lijianfu@lyu.edu.cn)

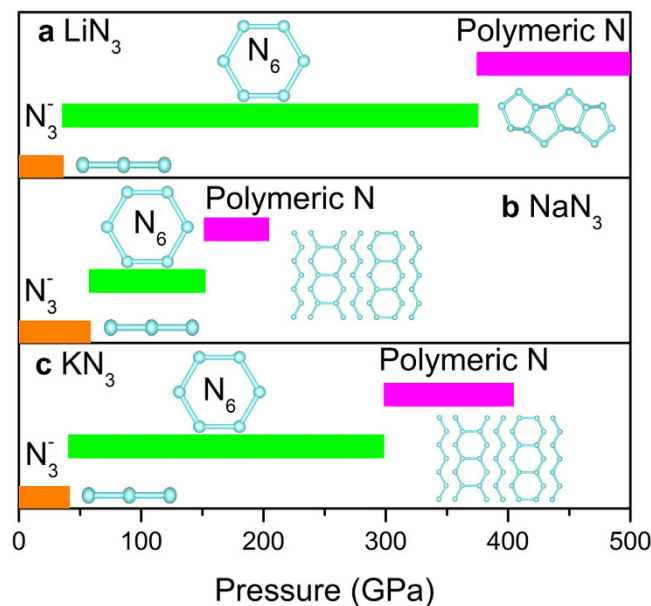


Figure 1. Structural evolution of N_3^- anion in alkali metal azides under compression. (a) LiN_3 , (b) NaN_3 , and (c) KN_3 . Transition pressure and structures are taken from reference LiN_3^4 , NaN_3^5 , and KN_3^7 , respectively.

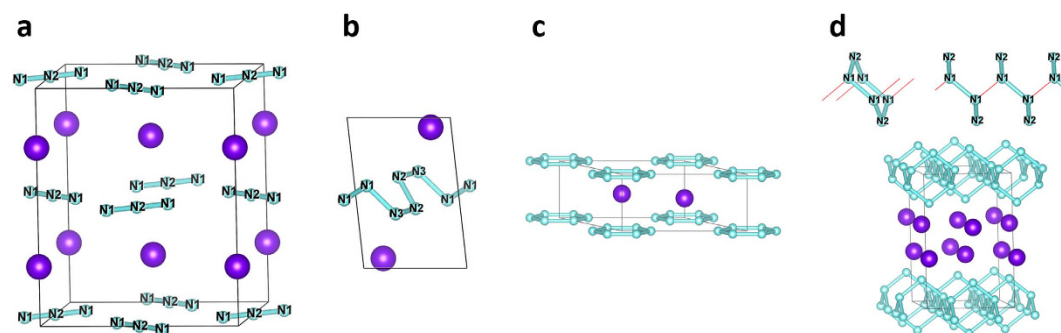


Figure 2. Crystal structures. The ambient condition and the predicted high-pressure phase: (a) $I4/mcm$; (b) $P-1$; (c) $P6/mmm$; and (d) $C2/m$. The large and small spheres denote rubidium and nitrogen atoms, respectively. The red lines denote the connection between N_6 rings in up section of (d). The nitrogen atoms in (a,b,d) have been labeled N1, N2, and N3 according to their Wyckoff positions.

evolution of N_3^- anions. It is helpful to investigate theoretically the pressure effect on rubidium azide and the role of rubidium atoms in the structural evolution process of N_3^- anions.

Under ambient conditions, α - RbN_3 has the lowest energy with a body-centered tetragonal (bct) lattice of space group $I4/mcm$, in which rubidium (Rb), nitrogen 1 (N1), and nitrogen 2 (N2) atoms are located on the 4a,4d, and 8h Wyckoff positions, respectively (Fig. 2a), which is isostructural to the low-temperature phase of KN_3 and CsN_3 in all respects²³. The nitrogen, linear and symmetric, occupy alternately $[0,1,1]$ and $[1\bar{1}0]$ directed position in the crystal forming planes ((001) and (002) planes) separated by layers of Rb ions. Recently, for the high-pressure behaviors of RbN_3 , we present the *in-situ* X-ray diffraction studies of RbN_3 up to 42.0 GPa at room temperature⁶. Two pressure-induced orientational phase transitions of α - RbN_3 ($I4/mcm$) \rightarrow γ - RbN_3 ($C2/m$) \rightarrow δ - RbN_3 were identified at 6.5 and 16.0 GPa, respectively.

In this work, we will focus on the structural evolution of anions under high pressure. A series of phase transitions in which N_3^- is converted to a chain like structure N_6 ring and layered polymeric nitrogen have been discovered up to 300 GPa by using a specifically developed particle swarm optimization (PSO) algorithm technique for crystal structure prediction²⁴. To confirm the thermal dynamic stabilities of new phases, phonon dispersion spectroscopies have been calculated. The electronic properties calculations indicate the $4d$ orbitals of Rb have been partially occupied in high-pressure phases and a strong hybridization has been formed between $4d$ orbital of Rb and $2p$ orbital of N in layered structure of RbN_3 .

Space group	Pressure (GPa)	Lattice parameters (Å, °)		Atom	Wyckoff positions	x	y	z
<i>I4/mcm</i>	0	a = 6.2871 (6.3098)	$\alpha = 90$	Rb	4a	0	0	0.25
		b = 6.2871 (6.3098)	$\beta = 90$	N1	8h	0.3664	0.1336	0
		c = 7.5106 (7.5188)	$\gamma = 90$	N2	4d	0.5	0	0
<i>P-1</i>	40	a = 3.3263	$\alpha = 96.7544$	Rb	2i	0.8007	0.9350	0.7555
		b = 4.7467	$\beta = 75.1448$	N1	2i	0.1171	0.5467	0.8935
		c = 5.5230	$\gamma = 97.8611$	N2	2i	0.4330	0.6051	0.4513
				N3	2i	0.6319	0.6399	0.2184
<i>P6/mmm</i>	100	a = 5.5482	$\alpha = 90$	Rb	2d	0.3333	0.6667	0.5
		b = 5.5482	$\beta = 90$	N	6j	0.7684	0.7684	0
		c = 5.5482	$\gamma = 120$					
<i>C2/m</i>	300	a = 3.9946	$\alpha = 90$	Rb	4i	0.2234	0	0.3843
		b = 4.0911	$\beta = 98.6538$	N1	8j	0.8612	0.2517	0.9327
		c = 6.1675	$\gamma = 90$	N2	4i	0.8201	0.5	0.8029

Table 1. The unit-cell parameters and atomic positions of the *I4/mcm*, *P-1*, *P6/mmm* and *C2/m* phase at 0 GPa, 40 GPa, 100 GPa and 300 GPa, respectively.

Computational Details

We have performed extensive structure searches to uncover the high-pressure structures of RbN_3 based on a global minimization of free-energy surfaces merging *ab initio* total energy calculations via PSO technique, as implemented in the Crystal Structure Analysis by Particle Swarm Optimization (CALYPSO) code^{24,25}. This method has successfully predicted the ground state structure for various systems including Nitrogen²⁶, Caesium²⁷, and superhard carbon nitride²⁸. The underlying *ab initio* structural relaxations and electronic band structure calculations are performed in the framework of density functional theory within generalized gradient approximation Perdew-Burke-Ernzerhof (GGA-PBE)²⁹, as implemented in the VASP code³⁰. The projector augmented wave (PAW)³¹ pseudopotentials are adopted with the PAW potentials taken from the VASP library where $4p^65s^1$ and $2s^22p^3$ are treated as valence electrons for Rb and N atoms, respectively. The cutoff energy (800 eV) for the expansion of the wave function into plane waves and Monkhorst-Pack³² *k*-meshes (*k*-points density 0.03 \AA^{-1}) are chosen to ensure that all the enthalpy calculations are well converged to better than 1 meV/atom. The calculations of net charge are based on Bader analysis^{33,34}. The phonon calculations are carried out by using a supercell approach as implemented in the PHONOPY code³⁵.

Results and Discussion

The variable-cell high-pressure structure predictions have been performed within a pressure region from 0 to 300 GPa, with system containing from one to eight formula units per simulation cell as implemented in CALYPSO code. Our structural searches identified not only the ambient conditions phase *I4/mcm* shown in Fig. 2a, three new structures are also depicted in Fig. 2b,d. The lattice constants of predicted structure at ambient pressure $a = 6.2871 \text{ \AA}$ and $c = 7.5106 \text{ \AA}$ are in agreement with the results obtained in experiment ($a = 6.3098 \text{ \AA}$ and $c = 7.5188 \text{ \AA}$)²³ which validates our computational method adopted here. The N_3^- ions are linear and symmetric, and the bond length of $\text{N}=\text{N}$ is 1.187 \AA , which is same as that in potassium azides and well in agreement with the experimental results (1.176 \AA)²³. The calculated atomic fractional coordinates are summarized in Table 1. The results indicate that N_3^- anions undergo transition of $\text{N}_3^- \rightarrow \text{N}$ chain $\rightarrow \text{N}_6$ ring \rightarrow layered N. Different from converting directly into N_6 ring structure in LiN_3 ^{4,8}, NaN_3 ^{5,8}, and KN_3 ^{7,9}, N_3^- anions translate to chain-like structure, which appears in CsN_3 ¹⁰ at 51 GPa, before entering N_6 ring structure. The layered nitrogen in *C2/m* phase is constructed by chair-like N_6 rings, as shown in up section of Fig. 2d, completely different from the high-pressure structures in LiN_3 ⁴, NaN_3 ⁵, and KN_3 ⁷. In *C2/m* phase, nitrogen atoms have two nonequivalent sites 8j and 4i, respectively. The nitrogen atom located on 8j site is connected with three neighboring N through three N-N bonds and the N located on 4i site is connected with two neighboring N through two N-N bonds.

To investigate the energetic stabilities of RbN_3 compound under high pressure, we calculate the formation enthalpy relative to the *I4/mcm* structure of RbN_3 in a pressure range from 0 to 300 GPa, as shown in Fig. 3a. The most stable structure is a tetragonal phase with *I4/mcm* symmetry from ambient pressure which is then replaced by a lower-enthalpy *P-1* structure at 30 GPa. Above 50 GPa, a hexagonal structure with *P6/mmm* symmetry is favored over other structures and remains the lowest-enthalpy

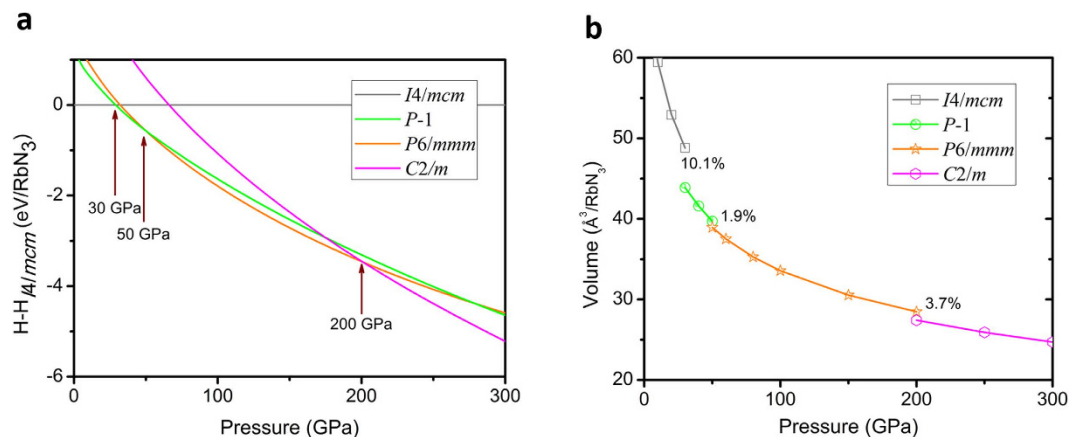


Figure 3. (a) Enthalpy of formation of selected structures of RbN₃ as a function of pressure (relative to the *I4/mcm* phase). (b) Phase diagram of RbN₃ at pressure region from 0 to 300 GPa.

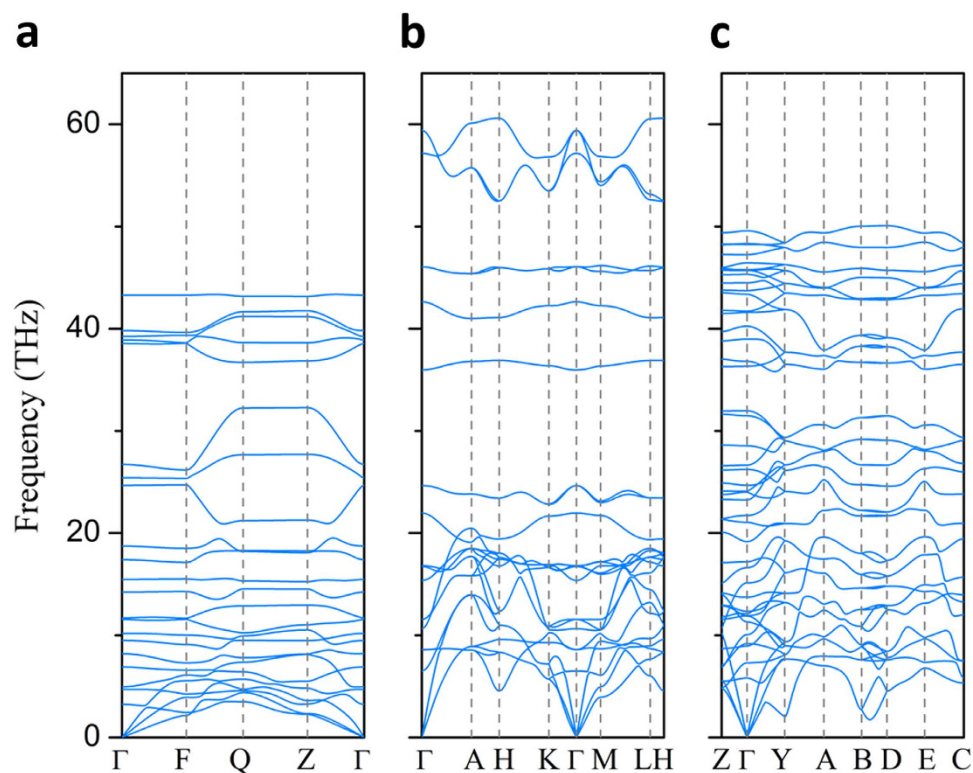


Figure 4. Phonon-dispersion curves of predicted structures. (a) *P-1*, (b) *P6/mmm*, and (c) *C2/m* at 40 GPa, 100 GPa and 300 GPa, respectively.

phase up to 200 GPa. Continuously increasing pressure, the RbN₃ will translate to a monoclinic structure with *C2/m* symmetry. Thorough structure searches using CALYPSO do not find any other structural change up to 300 GPa. The fact that the four structures are in entirely different crystal symmetry suggests that the transitions between them are first order which is indeed confirmed by the calculated P-V curves (Fig. 3b). The reductions of the volumes are found to be 10.1%, 1.9% and 3.7% for the transitions from *I4/mcm* to *P-1*, from *P-1* to *P6/mmm* and from *P6/mmm* to *C2/m*, respectively.

The dynamic stability of three predicted structures are examined by calculating the phonon spectra using the supercell method³⁵. No imaginary phonon frequency is found in the whole Brillouin zone at the pressure 40 GPa, 100 GPa and 300 GPa, respectively, as shown in Fig. 4.

Under pressure, the structural evolution of the rubidium azide is accompanied by the change of the electronic properties. To explore that, we calculated the electronic structures and their dependence on

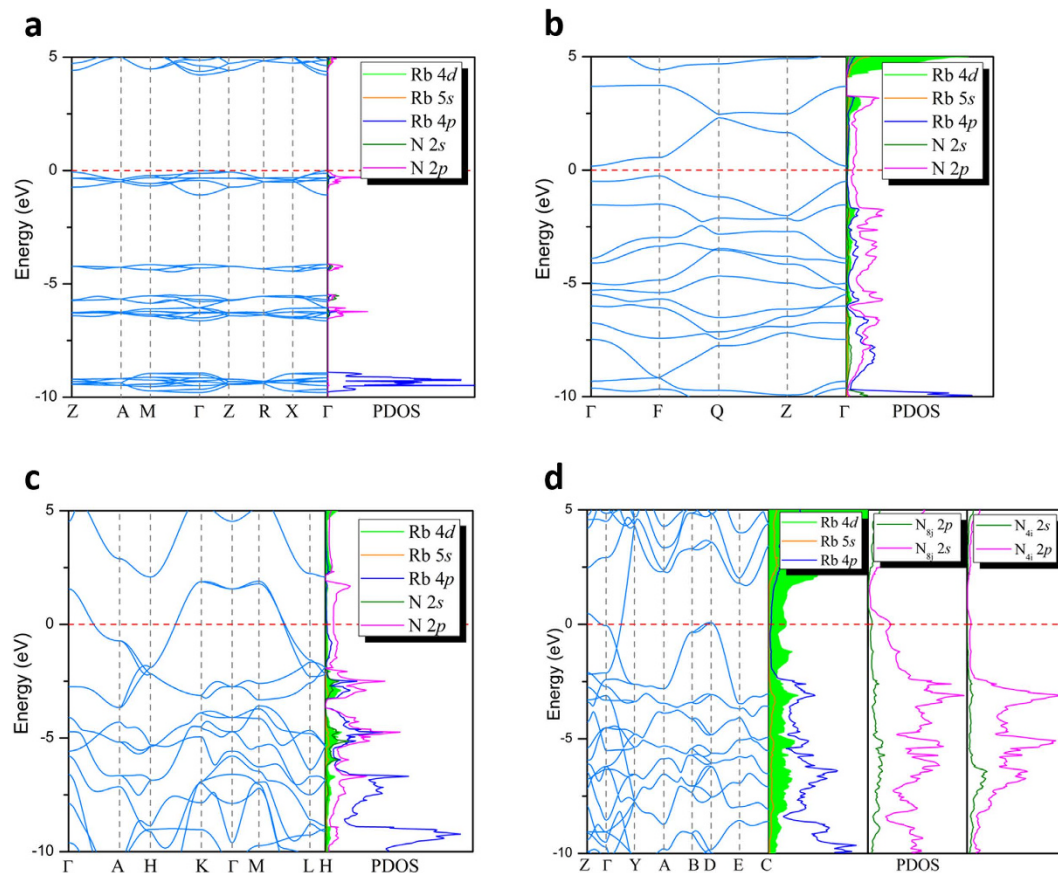


Figure 5. Band structure and projected density of states. (a) $I4/mcm$, (b) $P-1$, (c) $P6/mmm$, and (d) $C2/m$ at 0 GPa, 40 GPa, 100 GPa and 300 GPa, respectively. Dash line denotes Fermi energy level.

pressure in several aspects, including the electron localized functions (ELF), band structures, electronic band structure, projected density of states (PDOS), and net charge of Rb atoms.

As shown in Fig. 5, the four phase transitions of RbN_3 are accompanied by insulator-metal-metal transitions. At ambient conditions, the $I4/mcm$ structure is an insulator characterized by a large energy gap of 4.3 eV that is similar to the atmospheric pressure phases of other alkali metal azides^{7,10,12}. However, the $P-1$, $P6/mmm$ and $C2/m$ structures exhibit clear metallic behaviors by evidence of cross of band structures and the finite electronic DOS at the Fermi level. As can be seen from the partial DOS, $N-2p$ states contribute most to the valence band and the DOS near the Fermi level in $P-1$ and $P6/mmm$ structures. The detailed analysis for metallicity of $P-1$ and $P6/mmm$ can be found in previous works for CsN_3 ¹⁰ and KN_3 ^{7,9} due the similar electronic properties. For four considered structures, the strong covalent bonding between nitrogen atoms as well as the lone pairs electrons are revealed clearly by the ELF shown in Fig. 6. As pressure increase, the hybridization type between nitrogen atoms undergoes from sp (within $I4/mcm$) to sp^2 (within $P-1$ and $P6/mmm$), then to partial sp^3 (within $C2/m$).

More interestingly, the $4d$ orbital of rubidium is partially occupied in high-pressure phases as shown in Fig. 5b,d and there is an obvious orbital hybridization between the $4d$ of Rb and $2p$ of N located on $8j$ sites in $C2/m$ phase. To further confirm this result, we recalculate the PDOS of the four phases using a much small Wigner-Seitz radius, in which we change the spherical radius from defaults value in pseudo-potential (2.418 and 0.741 Å for Rb and N) to smaller values based on the Bader analysis, as shown in supplementary Figure S1-S3. The recalculated results are similar to the previous PDOS for the four phases except the value of densities. To study the impact of partial occupation of $4d$ orbital on electronic properties, we calculate the net charge of Rb atom based on Bader analysis, as shown in Fig. 7. At ambient conditions, the Rb atoms contribute almost one electron (0.85) to three N atoms forming N_3^- anion.

Under high pressure, the net charge decreases due to the partial occupation of $5d$ orbital, though the Rb atom still loses its $5s$ electron. Though the transition metal-like property of Rb elements has been reported by both experimental and theoretical works in alkali metal elements under high pressure³⁶⁻³⁸, there has been no research addressing that in chemical compounds. The difference that comes from the

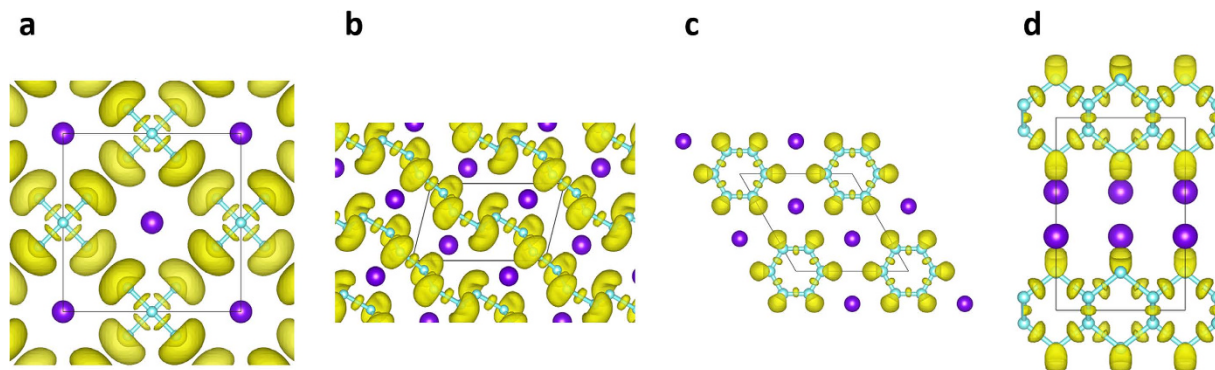


Figure 6. The electron localized functions. (a) $I4/mcm$, (b) $P-1$, (c) $P6/mmm$, and (d) $C2/m$ at 0 GPa, 40 GPa, 100 GPa and 300 GPa, respectively. The value of isosurface is 0.8.

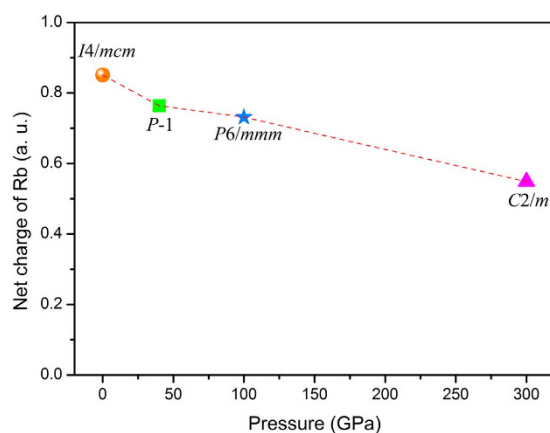


Figure 7. The net charge of Rb atoms based on Bader charge analysis for Rb in $I4/mcm$, $P-1$, $P6/mmm$ and $C2/m$ phases at 0 GPa, 40 GPa, 100 GPa and 300 GPa, respectively.

occupation of d orbitals is caused by the spd hybridization in alkali metal elements, for RbN_3 that results from the hybridization between $4d$ of Rb and $2p$ of N which may enhance the stability of compound.

Conclusion

In summary, we studied the evolution of the structures of RN_3 under high pressure by using an unbiased automatic structure search method based on first-principles total energy calculations and geometry optimization. We predicted three new high-pressure structures of RbN_3 with $P-1$, $P6/mmm$ and $C2/m$ structure at pressure of 30, 50 and 200 GPa. This result extends the high-pressure structures RbN_3 . The analysis of the electronic structure reveals that the transition trend of N_3^- ions from linear molecules to polymer chains, then to benzene-like rings, and finally to layered polymeric nitrogen is driven by the hybridization of N atoms in which the nitrogen hybridized types are sp , sp^2 , sp^2 , and partial sp^3 , respectively. For the first time, we reveal that the Rb atoms in RbN_3 possess obvious transition metal-like properties under high pressure. In $C2/m$ phase, a strong hybridization has been found between $4d$ orbitals of Rb and $2p$ orbitals of N.

References

- Fuith, A. The KSCN family: Structural properties and phase transitions of crystals with three-atomic linear anions. *Phase Transitions A Multimat. J.* **62**, 1–93 (1997).
- Evans, B. L., Yoffe, A. D. & Gray, P. Physics and chemistry of the inorganic azides. *Chem. Rev.* **59**, 515–564 (1959).
- Zhu, H. *et al.* Pressure-induced series of phase transitions in sodium azide. *J. Appl. Phys.* **113**, 033511 (2013).
- Wang, X. *et al.* Polymerization of nitrogen in lithium azide. *J. Chem. Phys.* **139**, 1–6 (2013).
- Zhang, M. *et al.* Structural and electronic properties of sodium azide at high pressure: A first principles study. *Solid State Commun.* **161**, 13–18 (2013).
- Li, D. *et al.* Pressure-induced phase transitions in rubidium azide: Studied by *in-situ* x-ray diffraction. *Appl. Phys. Lett.* **105**, 071903 (2014).
- Li, J. *et al.* Pressure-induced polymerization of nitrogen in potassium azides. *EPL (Europhysics Lett.)* **104**, 16005 (2013).

8. Zhang, M., Yan, H., Wei, Q., Wang, H. & Wu, Z. Novel high-pressure phase with pseudo-benzene 'N₆' molecule of LiN₃. *EPL (Europhysics Lett.)* **101**, 26004 (2013).
9. Zhang, J. & Zeng, Z., Lin, H.-Q. & Li, Y.-L. Pressure-induced planar N₆ rings in potassium azide. *Sci. Rep.* **4**, 4358 (2014).
10. Wang, X., Li, J., Zhu, H., Chen, L. & Lin, H. Polymerization of nitrogen in cesium azide under modest pressure. *J. Chem. Phys.* **141**, 044717 (2014).
11. Medvedev, S. *et al.* Phase stability of lithium azide at pressures up to 60 GPa. *J. Physics. Condens. Matter* **21**, 195404 (2009).
12. Babu, K. R., Lingam, C. B., Tewari, S. P. & Vaitheeswaran, G. High-pressure study of lithium azide from density-functional calculations. *J. Phys. Chem. A* **115**, 4521–9 (2011).
13. Huang, X. *et al.* Large volume collapse during pressure-induced phase transition in lithium amide. *J. Phys. Chem. C* **116**, 9744–9749 (2012).
14. Ramesh Babu, K., Vaitheeswaran, G. & Babu, K. R. Metal azides under pressure: An emerging class of high energy density materials. *J. Chem. Sci.* **124**, 1391–1398 (2012).
15. Prasad, D. L. V. K., Ashcroft, N. W. & Hoffmann, R. Evolving Structural Diversity and Metallicity in Compressed Lithium Azide. *J. Phys. Chem. C* **117**, 20838 (2013).
16. Eremets, M. I. *et al.* Polymerization of nitrogen in sodium azide. *J. Chem. Phys.* **120**, 10618–23 (2004).
17. Ji, C. *et al.* High pressure X-ray diffraction study of potassium azide. *J. Phys. Chem. Solids* **72**, 736–739 (2011).
18. Ramesh Babu, K. & Vaitheeswaran, G. Ab-initio study of structural and vibrational properties of KN₃ under pressure. *Chem. Phys. Lett.* **533**, 35–39 (2012).
19. Ji, C. *et al.* Pressure-induced phase transition in potassium azide up to 55 GPa. *J. Appl. Phys.* **111**, 112613 (2012).
20. Hou, D. *et al.* Phase transition and structure of silver azide at high pressure. *J. Appl. Phys.* **110**, 023524 (2011).
21. Hooper, J. & Zurek, E. High Pressure Potassium Polyhydrides: A Chemical Perspective. *J. Phys. Chem. C* **116**, 13322–13328 (2012).
22. Hou, D. *et al.* Series of phase transitions in cesium azide under high pressure studied by *in situ* x-ray diffraction. *Phys. Rev. B* **84**, 064127 (2011).
23. Müller, U. Crystal structure refinements of KN₃, RbN₃, CsN₃ and TiN₃. *Z. Anorg. Allg. Chem.* **392**, 159–166 (1972).
24. Wang, Y., Lv, J., Zhu, L. & Ma, Y. Crystal structure prediction via particle-swarm optimization. *Phys. Rev. B* **82**, 094116 (2010).
25. Wang, Y., Lv, J., Zhu, L. & Ma, Y. CALYPSO: A method for crystal structure prediction. *Comput. Phys. Commun.* **183**, 2063–2070 (2012).
26. Wang, X. *et al.* Cagelike Diamondoid Nitrogen at High Pressures. *Phys. Rev. Lett.* **109**, 175502 (2012).
27. Miao, M.-S. Caesium in high oxidation states and as a *p*-block element. *Nat. Chem.* **5**, 846–852 (2013).
28. Wang, X., Bao, K., Tian, F. & Meng, X. Cubic gauche-CN: A superhard metallic compound predicted via first-principles calculations. *J. Chem. Phys.* **133**, 044512 (2010).
29. Perdew, J., Burke, K. & Ernzerhof, M. Generalized Gradient Approximation Made Simple. *Phys. Rev. Lett.* **77**, 3865–3868 (1996).
30. Kresse, G. & Furthmüller, J. Efficient iterative schemes for ab initio total-energy calculations using a plane-wave basis set. *Phys. Rev. B* **54**, 11169–11186 (1996).
31. Blöchl, P. Projector augmented-wave method. *Phys. Rev. B* **50**, 17953–17979 (1994).
32. Monkhorst, H. J. & Pack, J. D. Special points for Brillouin-zone integrations. *Phys. Rev. A* **13**, 5188–5192 (1976).
33. Henkelman, G., Arnaldsson, A. & Jónsson, H. A fast and robust algorithm for Bader decomposition of charge density. *Comput. Mater. Sci.* **36**, 354–360 (2006).
34. Tang, W., Sanville, E. & Henkelman, G. A grid-based Bader analysis algorithm without lattice bias. *J. Phys. Condens. Matter* **21**, 084204 (2009).
35. The program Phonopy is available at <http://phonopy.sourceforge.net/>; the force constant matrix is determined by VASP.
36. Parker, L. J., Atou, T. & Badding, J. V. Transition Element-Like Chemistry for Potassium Under Pressure. *Science*. **273**, 95–97 (1996).
37. Ma, Y., Oganov, A. R. & Xie, Y. High-pressure structures of lithium, potassium, and rubidium predicted by an ab initio evolutionary algorithm. *Phys. Rev. B* **78**, 1–5 (2008).
38. Fabbri, G., Lim, J., Veiga, L. S. I., Haskel, D. & Schilling, J. S. Electronic and structural ground state of heavy alkali metals at high pressure. *Phys. Rev. B* **91**, 1–9 (2015).

Acknowledgements

This work was supported by the National Science Foundation of China under Grants Nos. 11147007, 11304139, 11304111, 11274151, 11404278 and NSAF U1230202, Natural Science Foundation of Shandong Province No. ZR2014JL005, and Key Disciplines of Condensed matter Physics of Linyi University.

Author Contributions

X.W. and J.L. conceived the research. X.W. carried out the calculations. J.L., X.W., N.X., Z.H., H.Z. and L.C. analyzed the data. X.W. and J.L. wrote the paper.

Additional Information

Supplementary information accompanies this paper at <http://www.nature.com/srep>

Competing financial interests: The authors declare no competing financial interests.

How to cite this article: Wang, X. *et al.* Layered polymeric nitrogen in RbN₃ at high pressures. *Sci. Rep.* **5**, 16677; doi: 10.1038/srep16677 (2015).



This work is licensed under a Creative Commons Attribution 4.0 International License. The images or other third party material in this article are included in the article's Creative Commons license, unless indicated otherwise in the credit line; if the material is not included under the Creative Commons license, users will need to obtain permission from the license holder to reproduce the material. To view a copy of this license, visit <http://creativecommons.org/licenses/by/4.0/>